

1           **Development and Testing Approach of the**  
2           **Novel Mack Clamp Contact Patch Mechanism**  
3

4   Alireza Yazdanshenas, P.E.<sup>1</sup>  
5   President and Owner of Bevel Edge LLC  
6   Richardson, TX 75080  
7   [alireza.yazdanshenas@thebeveledge.com](mailto:alireza.yazdanshenas@thebeveledge.com)  
8   ASME Membership ID: 103752954

9  
10   Shih-Feng Chou, PhD  
11   Associate Professor at The University of Texas at Tyler, Dep. of Mechanical Engineering  
12   3900 University Blvd. Tyler, TX 75799  
13   [schou@uttyler.edu](mailto:schou@uttyler.edu)

14  
15   Chung Hyun Goh, PhD  
16   Associate Professor at The University of Texas at Tyler, Dep. of Mechanical Engineering  
17   3900 University Blvd. Tyler, Tx 75799  
18   [cguh@uttyler.edu](mailto:cguh@uttyler.edu)  
19   ASME Membership ID: 100327156

20

21

---

<sup>1</sup> Alireza Yazdanshenas, P.E. [alireza.yazdanshenas@thebeveledge.com](mailto:alireza.yazdanshenas@thebeveledge.com)

## 22 INTRODUCTION AND BACKGORUND

23 In the realm of fitness and competitive barbell sports, one of the most critical pieces of  
24 equipment is the weight plate retention collar (WPRC), also known as a collar, clamp, or  
25 clip. These collars play a crucial role in ensuring that weight plates, loaded onto a barbell,  
26 stay securely in place to prevent any accidents or injuries, as demonstrated in Figure 1.



27  
28

Figure 1. Failed weight plate retention collar from repetitive use

29 The designs of most WPRCs have evolved from their industrial predecessors, which saw  
30 significant improvements only as recently as the 1900s [1,2]. Generally, WPRCs, along  
31 with their industrial counterparts, serve the simple function of maintaining their position  
32 on a barbell shaft by utilizing frictional forces to prevent any movement [3]. In a gym  
33 environment, various exercises such as snatches, cleans, and deadlifts often involve  
34 dropping the loaded barbell onto the floor, generating a substantial amount of kinetic  
35 energy. Due to the natural gap between the barbell sleeve and the weight plates, a

36 significant portion of this kinetic energy is transferred laterally to the WPRC, resulting in  
37 slippage, as depicted in Figure 1, and even complete failure.

38 To understand this issue better, it's important to note that WPRCs are often considered  
39 insignificant accessories by companies that supply gym and fitness equipment. This is  
40 largely because the revenue generated from WPRC sales is considerably smaller  
41 compared to other fitness equipment and devices on the market. Additionally, for many  
42 large companies, the cost of developing a high-quality WPRC outweighs the business  
43 benefits. Consequently, the competition in designing and producing reliable WPRCs is  
44 stifled by the oligopoly that controls the market and dominates most of the innovation in  
45 this space. Adding to this issue, gym owners often see WPRCs as an additional expense  
46 that doesn't significantly contribute to their revenue, further reducing the demand for  
47 firms to produce satisfactory WPRCs. As a result, participants, end-users, and even  
48 professional athletes are left with limited choices when it comes to WPRCs, most of which  
49 offer minimal performance, pose safety risks, and hinder athletic progress.

50 The most critical design aspect of a WPRC is undoubtedly the interaction between the  
51 WPRC and the barbell sleeve. This interaction fundamentally determines the quality and  
52 user experience of a WPRC by providing resistance against weight plate sliding. In this  
53 paper, we present a novel WPRC design, the Mack Clamps, which addresses the most  
54 significant criteria for WPRCs “resistance to sliding” by utilizing optimized Contact Patches  
55 (CPs), as shown in Figure 2.

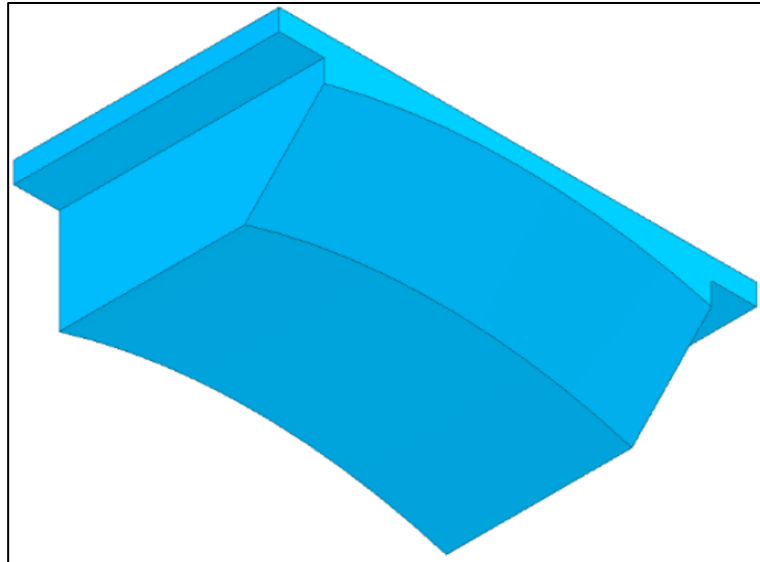


Figure 2. Contact patch CAD model

56  
57

58 While the Mack Clamps, as depicted in Figure 3, incorporate several newly integrated  
59 technologies and innovations, the primary focus of this work will be on the design process  
60 and validation of the CPs, which have resulted in the strongest performance of any known  
61 WPRC.



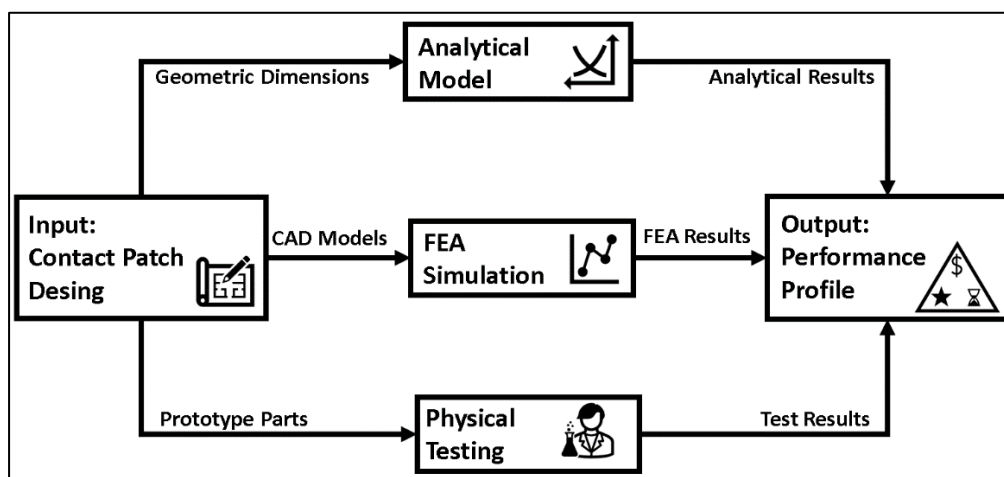
Figure 3. Embodiment of the Mack Clamps

62  
63

64

65 **Methodology**

66 The interaction between the barbell sleeve and any given WPRC essentially determines  
 67 the performance quality. This is not only crucial for recreational applications but can also  
 68 hold significance for industrial applications [4]. To validate this novel WPRC and assess  
 69 the tribological performance of the CPs, this work opted for a classical approach, as  
 70 depicted in Figure 4.



71  
72 Figure 4. Contact Patch validation approach

73 This approach encompassed three distinct steps. First, the critical geometry of the CPs  
 74 was analytically evaluated. Second, the CP function was simulated using Finite Element  
 75 Analysis (FEA). Third, prototype testing was conducted. The results from these three  
 76 independent methodologies were compiled and compared to validate the overall  
 77 performance profile of the Mack Clamps, with specific emphasis on the CPs.

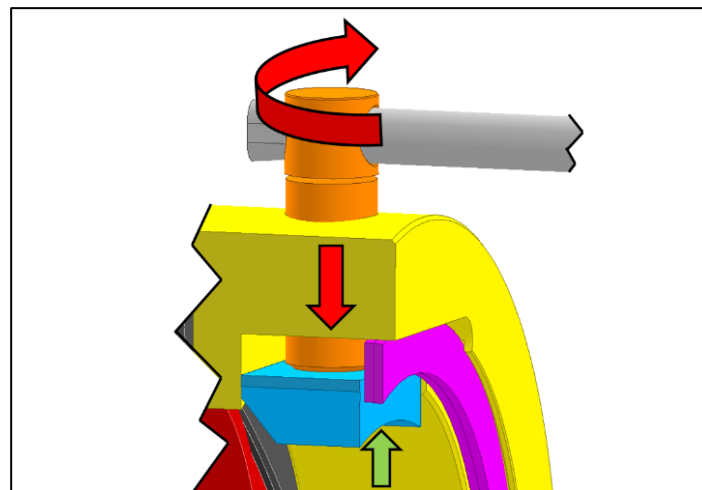
78 **Contact Patch Mechanism Design**

79 The primary objective of the CP mechanism was to provide users with a mechanical  
 80 advantage while maintaining simplicity with the fewest possible components. This

81 mechanical advantage is critical in the application of WPRCs, as they all adhere to a  
 82 common rule: the greater the clamping force, the better the collar's performance.  
 83 Therefore, the decision was made to employ the power screw mechanism to convert the  
 84 user's input torque into the necessary holding force for the CP mechanism, as represented  
 85 by Eq. 1:

$$T = \frac{Fd_m}{2} \left( \frac{L + \pi\mu d_m}{\pi d_m - \mu L} \right) + \frac{F\mu_c d_c}{2} \quad (1)$$

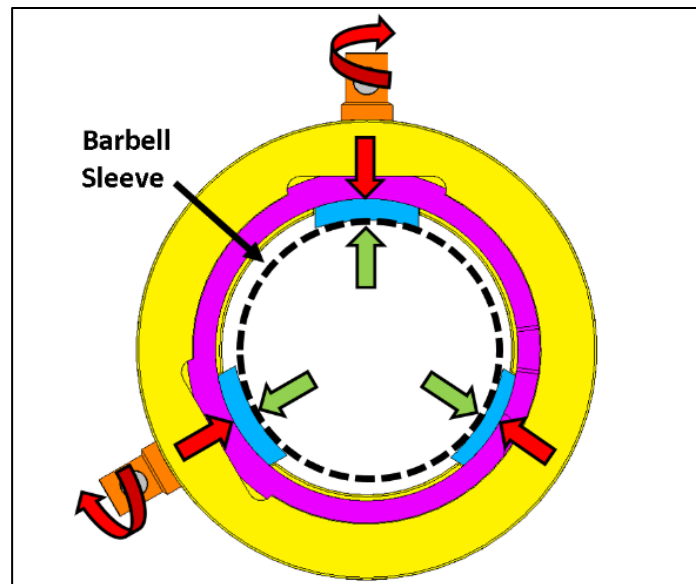
87 Figure 5 below depicts a cross-section of the Mack Clamp CAD assembly, illustrating the  
 88 general power screw mechanism. The user's input torque, denoted by the red curved  
 89 arrow, generates a clamping force against the CP, shown by the red straight arrow.  
 90 Additionally, equal and opposite reaction forces generated by the barbell sleeve are  
 91 represented by green arrows.



92 Figure 5 Contact Patch mechanism using the power screw concept  
 93

94 The selection of thread pitch and mating material for the thread was made to create a  
 95 self-locking thread, ensuring it remains secure during repetitions involving high impact  
 96 and vibrations while still allowing for a long lifecycle [5]. Furthermore, efforts were made

97 to minimize the frictional forces between the CP (blue components in Figure 5) and the  
98 screw (orange component in Figure 5) to enhance performance [6,7]. To further optimize  
99 the efficiency of the CP mechanism, the decision was made to triangulate the positions of  
100 the opposing contact patches. This triangulation allows the clamping load to disperse  
101 both vertically into the barbell sleeve and horizontally, creating an equal and opposite  
102 reaction from all three contact patches in the Mack Clamp design. This effect could be  
103 achieved using any axially symmetric arrangement of CPs; with three being the minimum  
104 number of contact patches needed to generate this effect.



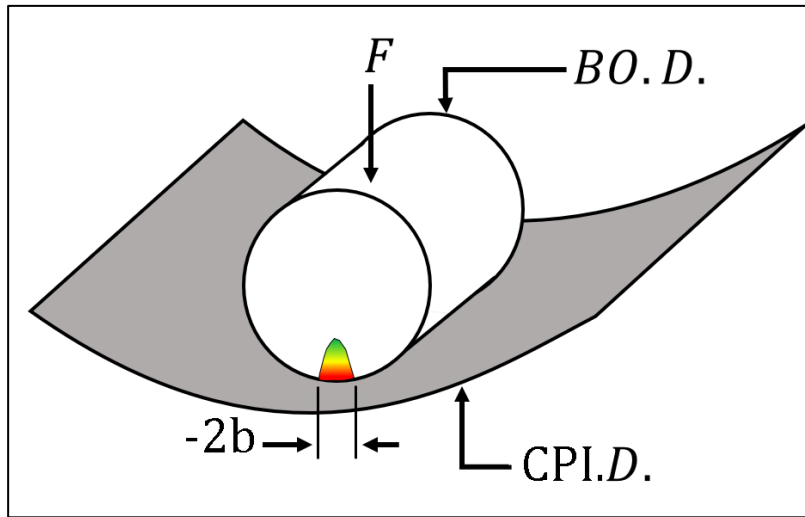
105  
106 Figure 6. Triangulation of the Contact Patches onto a given barbell sleeve

107 As shown in Figure 6, two dynamic contact patches apply force against a third stationary  
108 contact patch. The outer diameter of the barbell sleeve is represented by a dashed line,  
109 and the respective reaction forces are indicated by green arrows. This configuration  
110 ensures that the activation of any one of the turnbuckles automatically loads all three CPs  
111 equally and simultaneously. Furthermore, this arrangement simplifies the complexity of

112 the validation analysis, as it can be assumed that analysis of one CP will yield valid results  
 113 for the other two as well.

114 **Analytical Approach**

115 To maximize the grip between a CP and a barbell sleeve while minimizing stress, a concave  
 116 contact surface was chosen to mate with the cylindrical outer diameter (O.D.) of a  
 117 standard barbell sleeve [8,9]. This results in a traditional cylindrical mating surface pair,  
 118 illustrated in Figure 7.



119  
 120

Figure. 7 Hertzian contact of Barbell O.D. and Contact Patch I.D.

121 This cylindrical contact between two elastic solids, referred to as Hertzian Contact, can  
 122 be reliably analyzed and modeled using the Hertzian equations provided below. Equation  
 123 2 predicts the maximum pressure, while Equation 3 predicts the half-width of the contact  
 124 area.

125 
$$p_{max} = \frac{2F}{\pi bl} \quad (2)$$

126 
$$b = \sqrt{\frac{2F}{\pi l} \frac{(1 - \nu_1^2)/E_1 + (1 - \nu_2^2)/E_2}{1/(BO.D.) + 1/(CPI.D.)}} \quad (3)$$



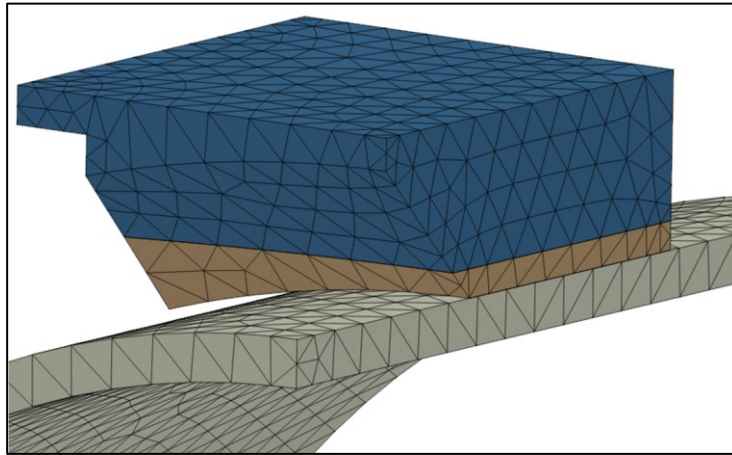
127 According to the Hertzian contact theory outlined above, the closer the inner diameter  
128 (I.D.) of the CP surface matches the O.D. of the barbell sleeve, the lower the stress  
129 concentration in the CP contact surface will be. This alignment could significantly enhance  
130 the performance of the CPs. However, when considering the entire contact patch  
131 mechanism along with the tolerances of all other components involved, achieving a close  
132 match between the CP I.D. and the barbell sleeve O.D. would require much tighter  
133 tolerances overall. Tightening the tolerances of all components involved significantly  
134 increases production costs. Through manual analytical iterations, it was determined that  
135 the ideal CP I.D. for this specific application should be 63.5 mm (2.5 in). Based on having  
136 the CPs at minimum design criteria with the loads at maximum operation levels, the  
137 Hertzian analytical model predicted a maximum contact stress of 651 Mpa (94.4 ksi) and  
138 a contact area width of about 2.54 mm (0.1 in).

### 139 **FEA Validation**

140 While the analytical modeling yielded favorable results for the direct contact surface,  
141 uncertainty still existed regarding the remaining aspects of the CP geometry. To address  
142 this, FEA was performed using the open-source software PrePoMax to identify any  
143 irregular or unexpected stress concentrations within the CP geometry [10]. To optimize  
144 the simulation's processing time, several strategic adjustments were made to the  
145 simulation model.

146 First, the symmetrical properties of the CP mechanism were leveraged to enable the  
147 simulation to be divided in half, as illustrated in Figure 8. Appropriate boundary conditions

148 and forces were applied to create the most realistic scenario. Using a single partition  
149 enhanced the accuracy of the contact surface while ensuring uniformity in the CP's  
150 irregularly shaped features. Given the well-established and reliable analytical model for  
151 Hertzian contact in this scenario, an autogenerated mesh with maximum element sizes  
152 up to 1.27 mm (0.05 in) was employed to further reduce calculation time and load.



153  
154

Figure. 8 PrePoMax FEA simulation set up for the Contact Patches

155 As anticipated, the results of the static FEA analysis closely mirrored those of the  
156 analytical model [11], with a maximum Von Mises stress of 637.8 MPa (92.5 ksi)  
157 concentrated along the center of the contact area, as indicated in Figure 9. This slight  
158 variation from the analytical model is attributed to the differences in the CP geometry, a  
159 factor the analytical model cannot account for. More crucially, no unexpected stress  
160 concentrations were detected due to the edges, corners, and tapers incorporated into  
161 the CP geometry.

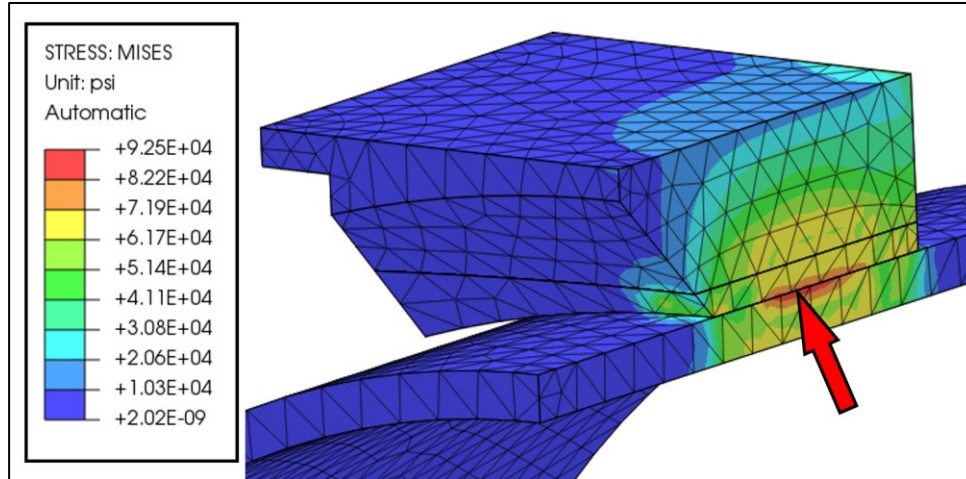


Figure. 9 PrePoMax FEA results showing Von Mesis stress concentration

162  
163

164 Moreover, the FEA model, as depicted in Figure 10, suggested a contact deformation  
 165 width of approximately 2.54 mm (0.1 in). These results not only reaffirmed congruence  
 166 with the analytical model but also provided the necessary confidence to proceed to the  
 167 prototyping and testing stage of this project.

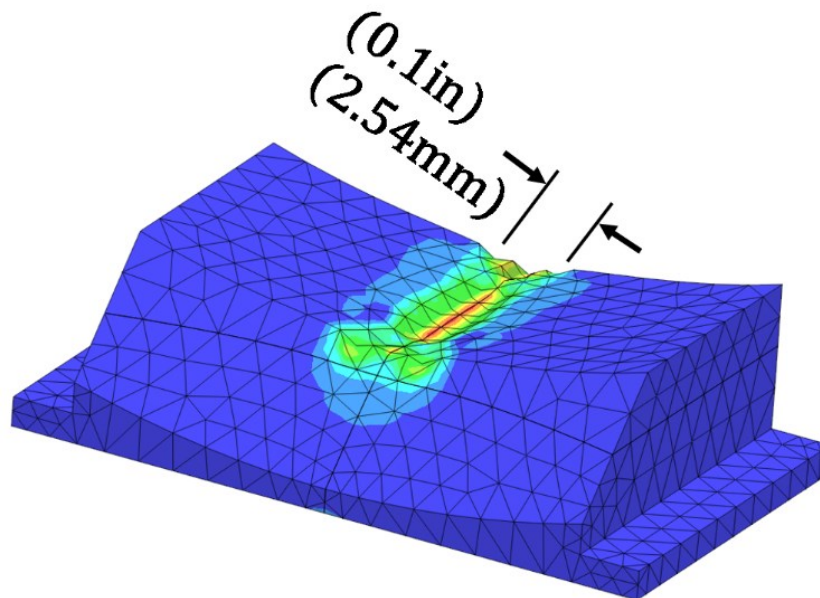


Figure. 10 PrePoMax FEA results showing deformation as a scale factor of 80

168  
169

170

171

172 **Engineering Testing**

173 *Purpose and Scope of Testing*

174 Once the theoretical and computational approaches of CP design provided convergent  
175 results, the natural progression was to validate the physical CP performance. To achieve  
176 the irregular CP geometry and induce natural surface roughness for enhanced holding  
177 force [12], casting was chosen as the manufacturing method instead of machining to  
178 further reduce costs and manufacturing time. However, concerns arose about the  
179 material properties and porosity of cast components. If the cast CPs did not closely meet  
180 the material specifications, it would significantly impact their ability to grip a barbell  
181 sleeve, potentially necessitating changes in the planned manufacturing approach.  
182 Validation testing was deemed necessary to ensure that the casting process for CPs met  
183 the specific engineering / material requirements. The testing scope focused on CP  
184 hardness and CP function to validate the holding force of this novel WPRC.

185 *Testing Setup*

186 First, test coupons from the production batch underwent hardness testing according to  
187 standard procedures, as shown in Figure 11, to verify that the CP material properties met  
188 the required specifications [13].

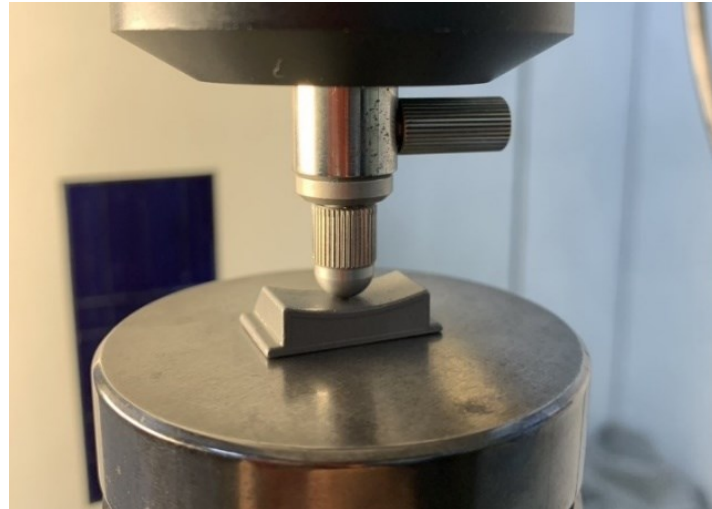


Figure 11. Rockwell-B hardness testing of the CP

189  
190

191 Second, a unique testing setup for WPRC was implemented to measure the holding force  
192 performance of the Mack Clamps using the novel CP mechanism. Figure 12 illustrates the  
193 WPRC testing setup using a universal material testing machine. In the diagram,  
194 component 1 is the coupling adopter connecting the modified barbell sleeve to the load  
195 cell. Component 2 represents the third-party barbell sleeve, while component 3 is a third-  
196 party cast iron Olympic weight plate, and component 4 is a base made of simple alloy  
197 steel tubing.

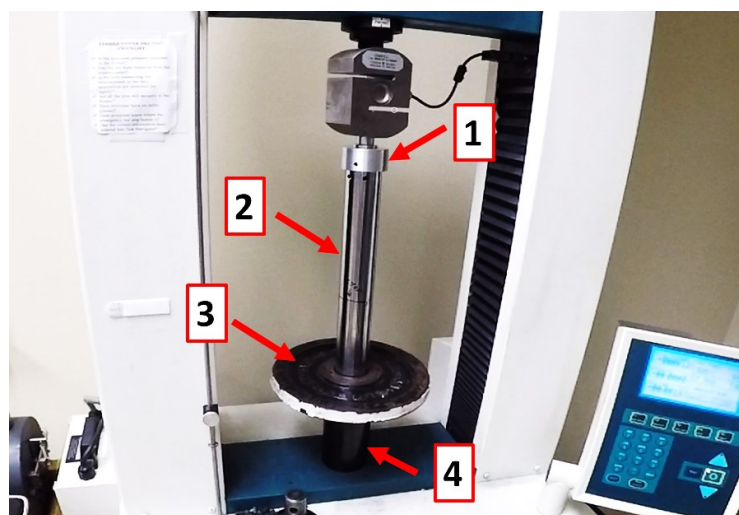


Figure 12. Weight plate retention collar setup

198  
199

200 This testing setup deliberately restricts the physical interaction of the Mack Clamps to  
201 only third-party components, namely the barbell sleeve and the Olympic weight plate.  
202 This decision was made for two key reasons: to maintain objectivity and realism while  
203 testing the Mack Clamps and CP mechanism and to allow others to replicate this testing  
204 using publicly available components that are critical to the setup. A detailed engineering  
205 drawing of this testing setup, with the corresponding numbers, is also provided in  
206 Appendix A for further reference.

207 Testing Procedure

208 For this testing, a Tinius Olsen H100K-S model was employed, operating at a speed of 150  
209  $\pm 30$  mm/min ( $0.05 \pm 0.1$  ft/min) in accordance with ASTM D1894 standard for all test  
210 trials. Although ASTM D1894 was initially developed for determining the coefficient of  
211 friction between two surfaces, it was assumed that this machine travel speed would be  
212 suitable for barbell clamp testing, as the frictional force is what keeps the clamp securely  
213 in place against the barbell sleeve. Given that this testing is the first of its kind, no other  
214 reference existed for testing WPRC.

215 Initially, the complete assembly of the Mack Clamps was evaluated based on the  
216 categories listed in Table 1.

217

Category	Value
Claimed Weight	0.454 kg (1.0 lb)
Actual Weight	0.467 kg (1.03 lb)
Full Engagement Length Distance	11.6 mm (0.455 in)
Fit on 1.9" O.D. Bar	Yes
Serviceable	Yes
Shock Absorbing	Yes
Rotational Degree of Freedom	Yes
Contact Surface Material	Alloy Steel

218

Table 1. Mack Clamp pretesting evaluation

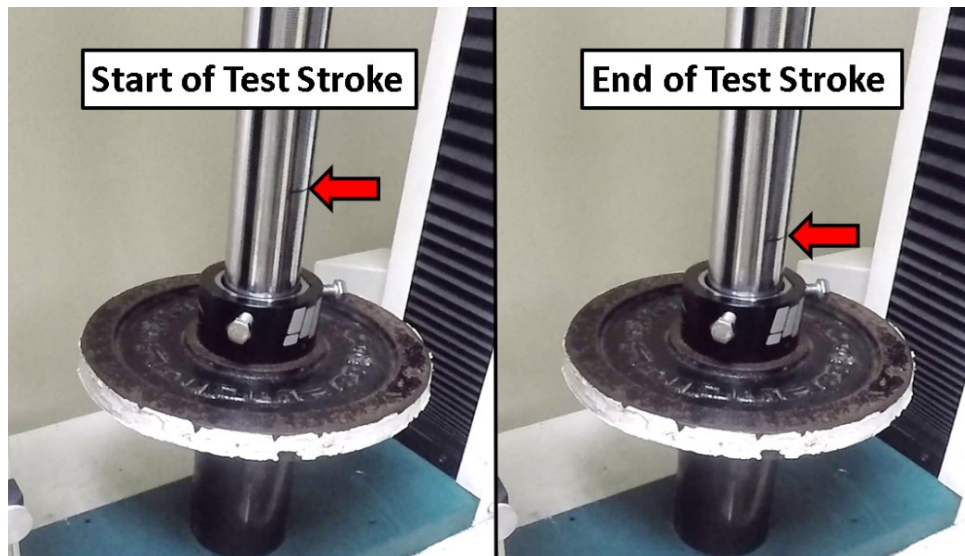
219 To focus on CP performance, the Dynamic Shock absorption system of the Mack Clamps  
 220 was disassembled and set aside. This was done to prevent the shock absorption system  
 221 from interfering with the extracted load vs. distance graphs. Next, two hex screws of the  
 222 same size and thread pitch (3/8-16 UNC) were used to replace the original screw handles  
 223 to apply reliable and repeatable torque to the CP mechanism. The 3/8-16 UNC hex screws  
 224 were lubricated with Rapid Tap to reduce the effects of thread friction. Torque was  
 225 applied to the CP mechanism using the AC Delco torque wrench to tighten the collar  
 226 against the barbell sleeve, as shown in Figure 13.



227  
228

Figure 13. Installation of the Mack Clamps using a torque wrench

229 Both hex screws were torqued to the required test trial values. This process was repeated  
230 for all other torque values: 6.7, 13.5, 20.0, and 27.1 N-m (5, 10, 15, and 20 ft-lb). When  
231 the desired input torque was applied, the machine stroke was activated simultaneously  
232 with the data acquisition sensors. The machine stroked the clamp against the weight plate  
233 until a slip between the barbell sleeve and the WPRC occurred. After detecting slipping,  
234 the machine continued its stroke at the given input speed for another 10-33 mm (.39-1.18  
235 in) before being manually stopped. Figure 14 displays the stroke of the barbell sleeve  
236 during a single test run by indicating the movement of a line mark on the barbell sleeve.



237  
238

Figure 14. Test stroke of the Mack Clamp testing process

239 Between trial runs, a visual inspection was conducted on the barbell clamp CPs and the  
240 barbell sleeve to ensure no significant damage occurred. The barbell sleeve was brushed  
241 down with a plastic brush to remove potential debris. This process was repeated 3-5 times  
242 for each specified torque value per testing procedure.



243 As a final set of tests, the original torque handles of the CP mechanism were reinstalled  
244 and hand-tightened with maximal effort. Since the Mack Clamps and the CP mechanism  
245 are designed to work purely by hand, it was crucial to determine the holding force against  
246 the barbell sleeve using a hand-tight input torque. Hence, 4 sets of hand-tight torque  
247 testing were performed to account for variability. While hand-tight torque may not  
248 provide scientific reliability, it was essential to obtain a ballpark estimate of what is  
249 realistically achievable by hand compared to a torque wrench.

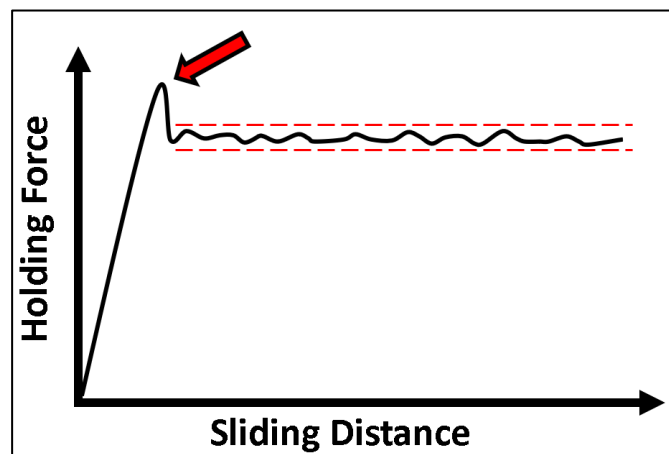
250

251 **Test Results**

252 Overall, the testing results align with expectations, primarily due to the simplicity of the  
253 CP mechanism design and adherence to common engineering principles.

254 **Testing data**

255 Data from the load cell was compiled and graphed to visualize the interaction between  
256 the CP mechanism and the barbell sleeve. A clear trend emerged once the testing data  
257 was plotted, as shown in Figure 15. The holding force of the CPs against the barbell sleeve  
258 exhibited a linear increase with the stroke of the testing machine, followed by a peak and  
259 a sudden drop. The peak represents the maximum static holding force provided by the  
260 CP, determined by the input torque and the static coefficient of friction. Subsequent  
261 fluctuations in sliding holding force remained within a consistent range, closely related to  
262 the CP dynamic coefficient of friction [14].



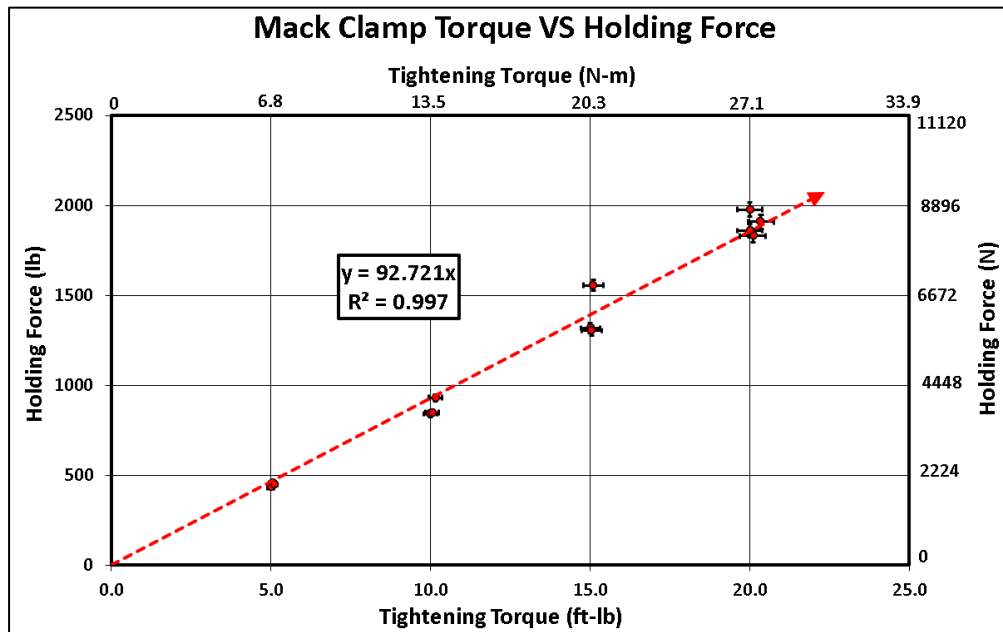
263  
264

Figure 15. General form of Mack Clamp Contact Patch testing data

265 For each test run, the peak holding force highlighted in Figure 15 was recorded as the  
266 single data point representing the respective trial. The compiled graphs of each test run  
267 can be found in Appendix A for further reference.

268 Interpolated performance graph

269 To offer a comprehensive representation of CP performance, a graph plotting each peak  
 270 holding force extracted against the corresponding CP mechanism tightening torque was  
 271 created. The resulting graph, displayed in Graph 1, serves as the most objective and  
 272 concise reference to convey the Mack Clamp CP mechanism's performance.



273  
 274

Graph 1. Tightening Torque VS Holding Force of the Mack Clamps

275 The data points in Graph 1 feature a 1% maximum error for both holding force measured  
 276 by the Tinius Olsen load cell and the tightening torque applied by the AC Delco torque  
 277 wrench, as indicated by the respective error bars. The trend line, which originates from  
 278 the origin (y-intercept at zero),  $Y=92.721X$ , interpolates the theoretical expected holding  
 279 force of the CP mechanism concerning the applied tightening torque of both handles /  
 280 turnbuckles. It's important to note that due to physical material limits, this interpolation  
 281 cannot extend indefinitely. High enough tightening torque may cause deformations in the

282 CP mechanism components and cause a deviation from the trend line. Therefore, it is not  
283 recommended to interpolate the holding force beyond 61 N-m (45 ft-lb).

284 Peak Performance

285 While torque input using a torque wrench provided an objective and reliable baseline for  
286 evaluating the Mack Clamp and CP performance, it may not fully reflect the real-world  
287 performance when tightened by hand. The CP mechanism was designed for users to  
288 hand-tighten the Mack Clamps with, and using a torque wrench could result in an  
289 unrealistic scenario with extremely high input torque, which might not be feasible by  
290 hand. Thus, a series of hand-tightened tests were conducted toward the end of the testing  
291 to assess the expected peak performance.

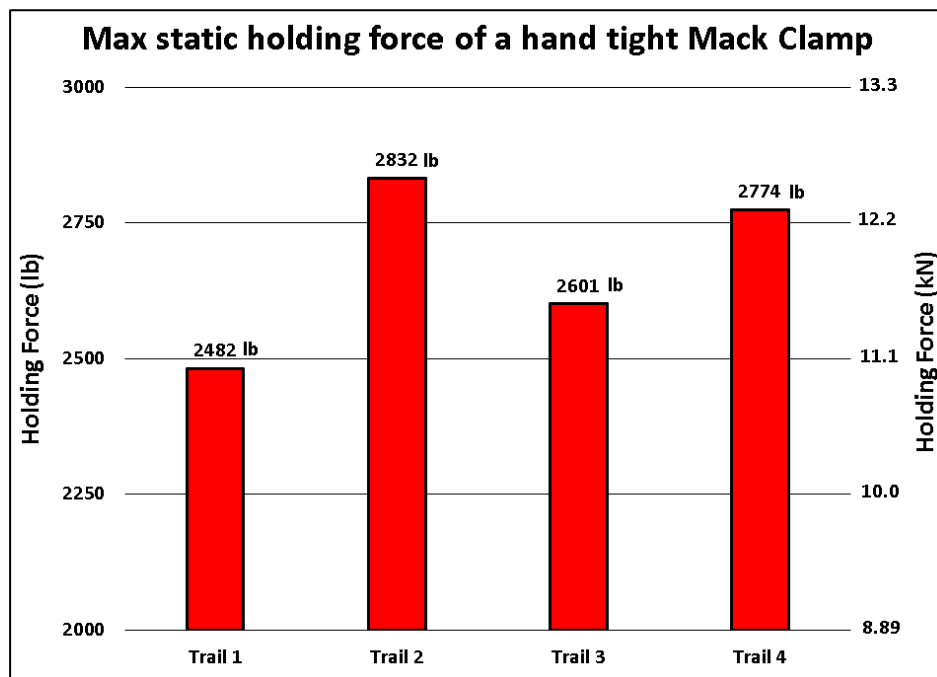


Chart 1. Maximum static holding force of a hand tight Mack Clamp

292  
293

294 Based on the testing results displayed in Chart 1, it can be concluded that the CP  
295 mechanism is efficient enough for a mid-level athlete to achieve a peak holding force of

296 up to 12.6 kN (2832 lb) from the Mack Clamps when hand-tightened. The average hand-  
297 tightened holding force was 11.9 kN (2672 lb), with the lowest result at 11.0 kN (2482 lb).  
298 These findings suggest that the Mack Clamps can be labeled as "The World's Strongest  
299 Barbell Collar" and "The Strongest Barbell Collar Ever Made." Furthermore, based on  
300 these results, it is estimated that the Mack Clamps, utilizing the CP mechanism, offer a  
301 peak performance twice as high as any existing barbell collar currently available on the  
302 market.

### 303 **Contact Patch Performance Profile**

304 Based on the design information obtained through analytical modeling, numeric  
305 modeling, and engineering testing, a performance profile for the Contact Patches (CPs)  
306 was established. Three primary criteria were taken into account to create this  
307 performance profile: manufacturing cost, peak strength, and endurance. These three  
308 criteria are considered fundamental in summarizing the performance of the CP design  
309 and, by extension, any WPRC in general.

310 An ideal performance profile would thus achieve a balance between Manufacturing Cost,  
311 Peak Strength, and Endurance, as depicted in Figure 16.

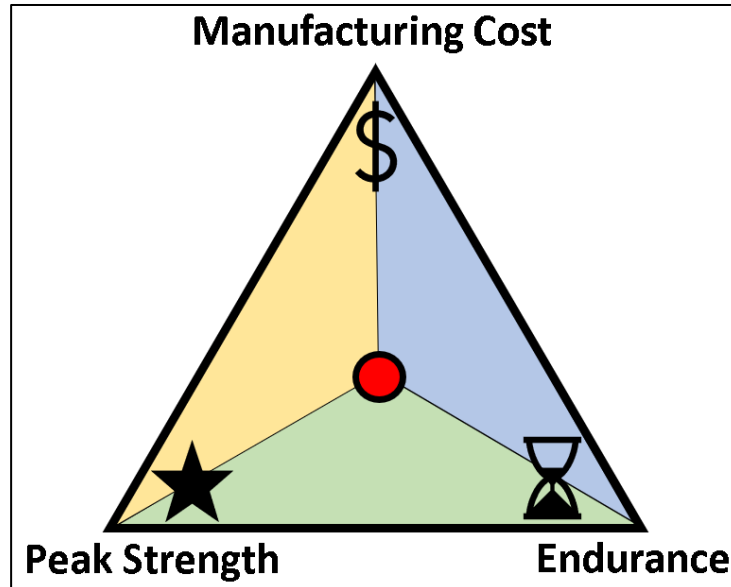


Figure 16. Ideally balanced Performance Profile of a given Contact Patch

312  
313

314 Manufacturing Cost

315 The CP faces significant demands as it must serve multiple functions and withstand  
316 extreme loads simultaneously. Typically, such high-performance requirements  
317 necessitate strict control of material properties and tight geometric tolerances, leading  
318 to a substantial increase in manufacturing costs. These demands usually preclude the  
319 possibility of casting the product. However, due to the specific steel alloy selection and  
320 secondary heat treatment options, casting was made feasible for manufacturing while  
321 still meeting stringent engineering requirements, resulting in cost-effective production of  
322 CPs.

323 Peak Strength

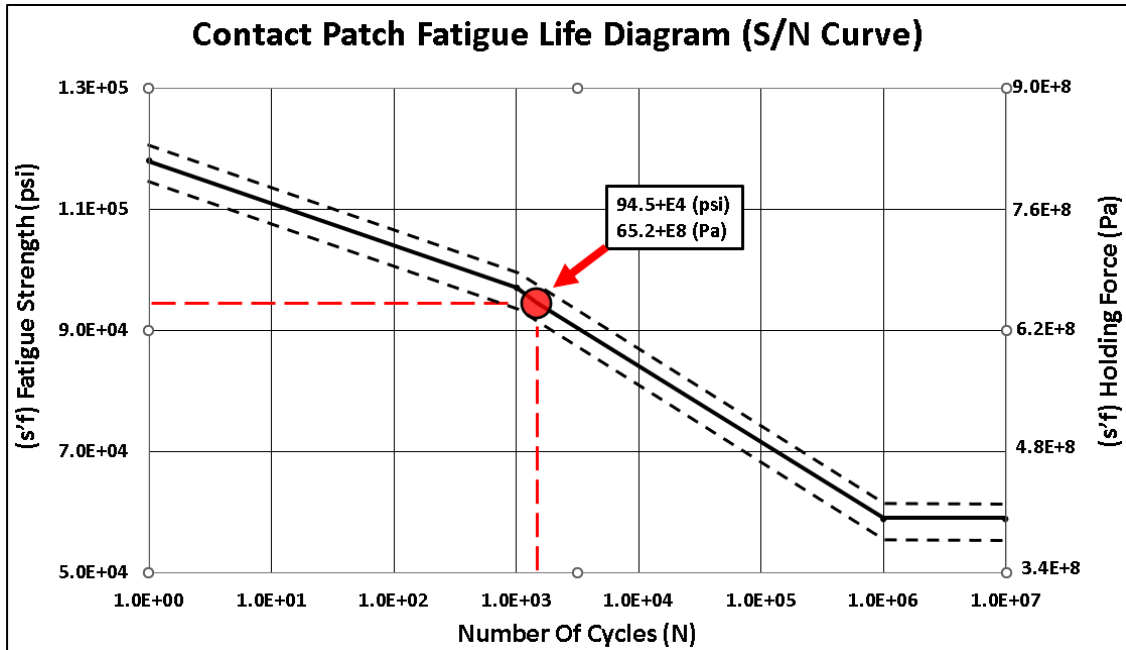
324 The paramount objective of developing Mack Clamps was to introduce a WPRC with  
325 significant strength that could make a substantial impact in the strength training  
326 community. The CPs' peak strength was the primary focus of this product development,

327 and based on the gathered data, it is reasonable to conclude that Mack Clamps possess  
328 unrivaled peak strength in the WPRC category. This remarkable peak strength is achieved  
329 through CP performance initiated by the CP mechanism as a whole. Although there is  
330 room for further enhancing CP strength, it would come at the cost of either increased  
331 manufacturing cost or a reduction in performance endurance.

332 Endurance

333 While peak strength is a top priority for the CP, endurance is also crucial to the product's  
334 end-users because it defines its utility. To optimize peak strength and reduce  
335 manufacturing costs, it was decided to sacrifice the endurance performance of the CPs.  
336 The question remained as to how much of the CP's endurance strength should be  
337 sacrificed and what would constitute a reasonable minimum endurance profile.

338 Following internal discussions and consultations, it became evident that the CPs' fatigue  
339 life should at least fall into the high cycle fatigue region to ensure satisfactory service life.  
340 However, since there is a direct trade-off between peak performance and fatigue life, it  
341 was decided to optimize the material to be as close as possible to the short cycle fatigue  
342 limit. Based on material testing, analytical modeling, and the derived fatigue life diagram  
343 as shown in Graph 2, the CPs' fatigue life, at peak performance use, is estimated to be  
344 between 1000 to 2000 cycles.

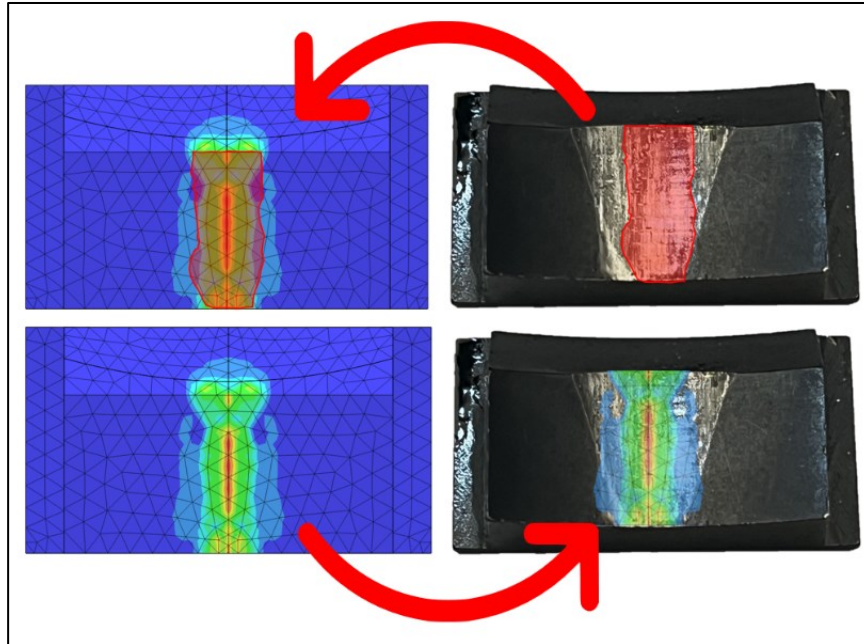


345  
346

Graph 2. Fatigue life analysis of CP though cyclical load at peak performance parameters

347 To further validate the estimation of cycle fatigue limit, a crude comparison of the FEA  
 348 results was made to the physically tested CPs. The highest worn regions of the physical  
 349 CPs were highlighted and overlaid to the FEA model for comparison. This highlighted  
 350 region does not include the removal of surface coating, but rather specifies the physical  
 351 wear observed. Vice versa, the highest stressed regions of the FA model were overlaid to  
 352 the physical CPs to further evaluate the comparison as shown in Fig. 17. This qualitative  
 353 comparison further improved the confidence of the CP endurance life.





354  
355

Figure 17. Over lay of physical testing and FEA simulation of the Contact Patches

356 Based on analytical results and the qualitative comparison, it is estimated that the CPs of  
357 the Mack Clamps can provide peak performance for approximately one year of use, and  
358 beyond that point, peak performance cannot be guaranteed. Nonetheless, the endurance  
359 of the CPs is expected to surpass that of any WPRC using rubber or plastic for contacting  
360 and gripping a barbell sleeve.

361 To compensate for the limited endurance of the CPs, the Mack Clamps feature  
362 serviceability within the CP mechanism design. This allows end-users to easily replace any  
363 worn-out CPs, ensuring extended peak performance.

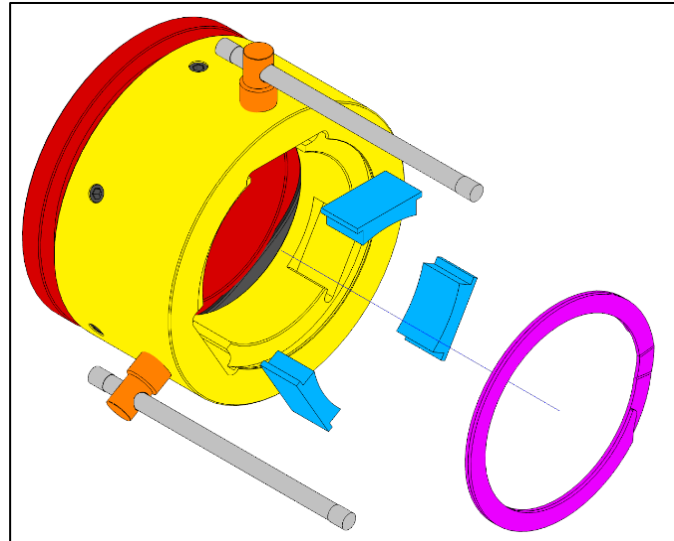


Figure 18. The serviceability and replacement of worn-out Contact Patches

364  
365

366 Contact Patch Performance Profile

367 Taking into account manufacturing cost, peak performance, and endurance, the  
368 performance profile of the CPs was evaluated to provide a realistic visual representation,  
369 as shown in Figure 19.

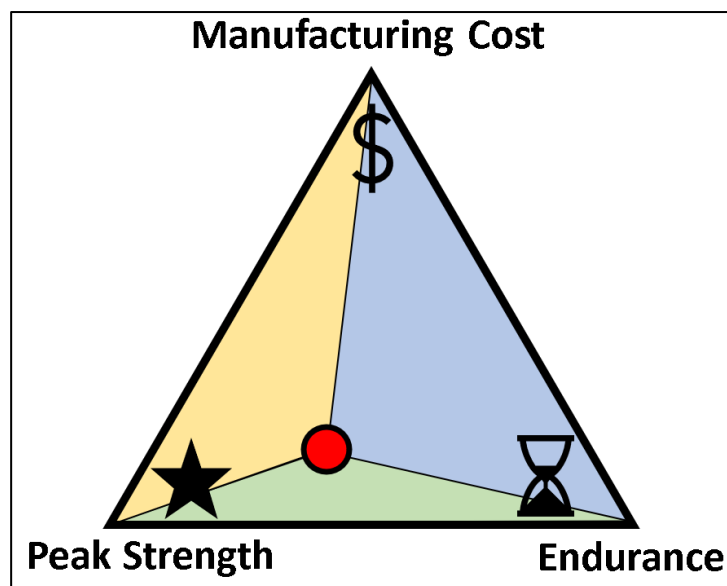


Figure 19. Derived Performance profile of the Mack Clamp Contact Patches

370  
371

372 As indicated by the red circle in the figure, manufacturing cost was significantly reduced  
373 through the casting method, while still achieving extremely high peak strength.  
374 Endurance of the CPs was the main sacrifice to attain exceptionally high peak  
375 performance with the given cost-effective production method. Overall, this performance  
376 profile was considered ideal for the Mack Clamps and the CP mechanism.

377

378 **Discussion**

379 **Testing Approach**

380 While this paper limited the testing of the CPs and the CP mechanism to the discussed  
381 testing setup, further field application testing was also conducted. However, due to  
382 limited resources, field and real-life application testing could not be performed with data  
383 acquisition and sensors. It is understood that field testing, in the end, is the best indicator  
384 of the specific performance demands of the CPs. With that said, no testing standard  
385 currently exists for the performance of WPRCs. Therefore, consensus would need to be  
386 reached on the most applicable and objective testing methodology. In general, it can be  
387 assumed that this testing setup, as described in the paper, has a direct and strong  
388 correlation to the field performance of the Mack Clamps and CPs.

389 Furthermore, it is believed, based on visual evidence, that the strong grip of the CP, in  
390 addition to the forced sliding, affected the surface properties of the given barbell sleeve.  
391 This means that as the testing continued, the surface of the barbell sleeve became  
392 smoother due to wear. This, in turn, could have reduced the maximum holding force  
393 capacity of the Mack Clamps towards the end of testing. This is something that could be  
394 solved by having multiple barbell sleeves available as replacements. However, in this  
395 instance, no replacement was available, and testing continued with the same provided  
396 specimen.

397

398 **Endurance**

399 As discussed in the “Contact Patch Performance Profile” section of this paper, the weakest  
400 point of the CP design is its endurance. However, it is important to note that the  
401 endurance of the CPs is relative to other components traditionally design and  
402 manufacture out of steel. In other words, when directly comparing the CP's performance  
403 to that of other WPRCs, it can be said with great confidence that the endurance of the CP  
404 is well beyond industry standards of WPRCs

405

406 **Future work**

407 **Mack Clamp comparison to other Weight Plate Retention Collars**

408 While the results obtained from the testing discussed in this paper strongly suggest that  
409 the Mack Clamps, with the CP mechanism, are the world's strongest WPRC, testing needs  
410 to be done to prove this objectively. As of the writing of this paper, testing is being  
411 conducted to compare the performance of the Mack Clamps to 12 other industry-leading  
412 WPRCs. The goal is to publish these findings as soon as possible to supplement claims and  
413 results found in this work specifically.

414 **Dynamic Shock Absorption and Rotational Degree of Freedom**

415 The Mack Clamps contain two more significant novel attributes: the Dynamic Shock  
416 Absorption System and the Rotational Degree of Freedom, which are outside the scope  
417 of this paper. While figures of these two concepts can be found in Appendix C, future  
418 work must be done to quantify and prove the performance and utility of these two  
419 integrated features objectively. Based on preliminary field testing, it is believed that these  
420 two novel features significantly aid the performance of the Mack Clamps and the CPs in  
421 general.

422 **Establishing design and testing standards for Weight Plate Retention Collars**

423 WPRCs play a vital role in athlete-safety and athlete-performance. While other critical  
424 strength equipment used are significantly overbuilt to prevent damage or injury, WPRCs  
425 are the only equipment that still regularly fail and pose significant risk. Therefore, future

426 work must be done to establish a working standard of WPRC design and WPRC testing to  
427 mitigate the risk of injury to strength athletes and their surrounding participants.

428 **Development and Testing of a 2.5kg Competition Grade Version**

429 Governing federations ask that the WPRC used in competition be exactly 2.5kg (5.5lb).

430 Therefore, to allow local, state, national, and international level competitions the ability

431 to use the Mack Clamps, a 2.5kg (5.5lb) standard version of the Mack Clamps must be

432 developed. This is a prioritized future goal of this ongoing project.

433

434 **ACKNOWLEDGMENT**

435 To complete this research, great and generous help was provided by the University of  
436 Texas at Tyler's Engineering Department under the leadership of Dr. Javier Kypuros. In  
437 addition, great and generous help was also provided by the University of Texas at Tyler's  
438 Mechanical Engineering Department under the leadership of Dr. Nael Barakat. This  
439 research could not have moved forward without their contribution. Next, the high-  
440 precision machining needed to rapidly prototype the test fixtures for this project was  
441 done by Mr. Edward Farina from the University of Texas at Tyler. His critical work is much  
442 appreciated. Furthermore, the third-party barbell sleeve for testing was generously  
443 provided by Mitch Stacey and Texas Power Bar. This donation allowed the testing to be  
444 conducted more objectively and realistically with the highest quality barbell possible.  
445 Also, gratitude and appreciation are extended all the way to Taiwan to our collaborative  
446 manufacturing partners Tim, and Chuck. It is with their help and teamwork that the  
447 manufacturing of the CP is possible to such a high standard. Lastly, a shoutout to  
448 PrePoMax and its founders for providing such a high-quality and easy-to-use open-source  
449 FEA program.

450



451 **NOMENCLATURE**

$T$	Input Torque by the user
$d_c$	Mean collar diameter
$d_m$	Mean thread diameter
$L$	Lead of the screw
$F$	Activation Force
$\mu$	Coefficient of friction for the thread
$\mu_c$	Coefficient of friction for the collar
$p_{max}$	Maximum contact pressure
$b$	Half width of contact area
$l$	Length of contact area
$\nu$	Poissons ration
$E$	Modulus of elasticity
$BO.D.$	Barbell Sleeve O.D. 50mm -1%
$CPI.D.$	Contact Path I.D. 2.5"±.005"

452

453

454 **REFERENCES**

- 455 [1] admin. 2020. “Evolution History of Shaft Collars and Select a Proper Shaft Collar -  
456 Fanovo Industries | Valve & Coupling Supplier.” May 29, 2020.  
457 [https://fanovo.com/industry-release/shaft-collar-evolution-](https://fanovo.com/industry-release/shaft-collar-evolution-history/#:~:text=Shaft%20collars%20saw%20few%20improvements)  
458 [history/#:~:text=Shaft%20collars%20saw%20few%20improvements](https://fanovo.com/industry-release/shaft-collar-evolution-history/#:~:text=Shaft%20collars%20saw%20few%20improvements).
- 459 [2] Ramsey, John, and Erwin Meyn. 1990. Review of POST CLAMP. Edited by National  
460 Aeronautics and Space Administration, issued August 1, 1990.  
461 <https://ntrs.nasa.gov/citations/19910005304>.
- 462 [3] “Axial Holding Power.” n.d. Stafford Manufacturing Corp.  
463 <https://www.staffordmfg.com/axial-holding-power/>.
- 464 [4] Wilson, Mark. 2002. Review of Shaft Collar Decisions Can Be Momentous. Edited by  
465 Amacoil Inc. Pffc-Online.com. pffc-online: Amacoil Inc. [https://www.pffc-](https://www.pffc-online.com/magazine/317-paper-shaft-collar-decisions)  
466 [online.com/magazine/317-paper-shaft-collar-decisions](https://www.pffc-online.com/magazine/317-paper-shaft-collar-decisions).
- 467 [5] E. Rabinowicz. 1971. “The Determination of the Compatibility of Metals through Static  
468 Friction Tests.” A S L E Transactions 14 (3): 198–205.  
469 <https://doi.org/10.1080/05698197108983243>.
- 470 [6] Litvin, Faydor, and John Coy. 1984. Review of Special Cases of Friction and  
471 Applications. Edited by National Aeronautics and Space Administration. Chicago,  
472 Illinois: American Society of Mechanical Engineering.
- 473 [7] Gaul, L., and R. Nitsche. 2001. “The Role of Friction in Mechanical Joints.” Applied  
474 Mechanics Reviews 54 (2): 93–106. <https://doi.org/10.1115/1.3097294>.

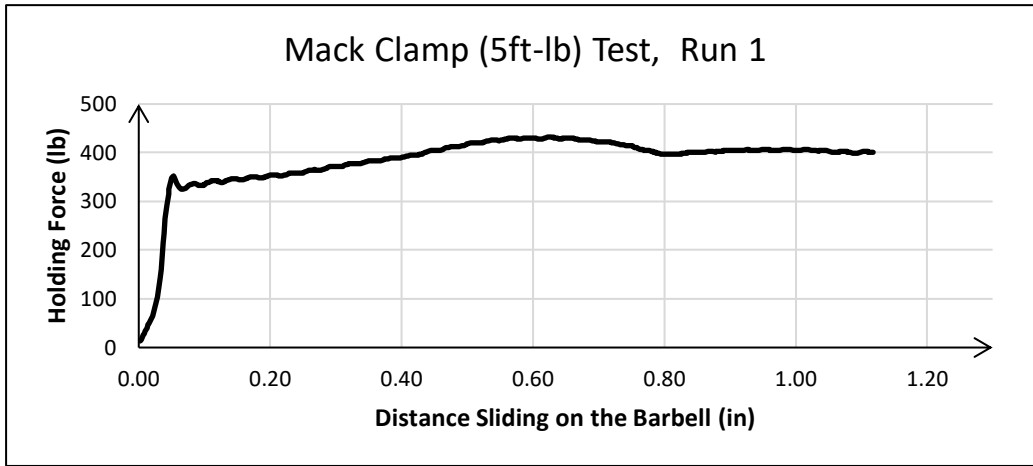
- 475 [8] Scholz, Christian, Dirk Spaltmann, and Mathias Woydt. 2011. "Slip-Rolling Resistance  
476 of Thin Films and High Toughness Steel Substrates under High Hertzian Contact  
477 Pressures." *Wear* 270 (7-8): 506–14. <https://doi.org/10.1016/j.wear.2011.01.005>.
- 478 [9] Francis, H A. 1971. "Interfacial Temperature Distribution within a Sliding Hertzian  
479 Contact." *A S L E Transactions* 14 (1): 41–54.  
480 <https://doi.org/10.1080/05698197108983226>.
- 481 [10] Fisher-Cripps, A. C. 1998. Review of The Hertzian Contact Surface. Edited by  
482 Department of Applied Physics, University of Technology. *JOURNAL of MATERIALS*  
483 *SCIENCE* 34 (July): 129–37.
- 484 [11] Bay, N., and T. Wanheim. 1975. Review of Real Area of Contact and Friction Stress  
485 at High Pressure Sliding Contact. Edited by Department of Mechanical Processing of  
486 Materials, AMT, Technical University of Denmark. *Wear* 38 (1976): 201–9.
- 487 [12] Yang, G.M, J.C Coquille, J.F Fontaine, and M Lambertin. 2001. "Influence of  
488 Roughness on Characteristics of Tight Interference Fit of a Shaft and a Hub."  
489 *International Journal of Solids and Structures* 38 (42-43): 7691–7701.  
490 [https://doi.org/10.1016/s0020-7683\(01\)00035-x](https://doi.org/10.1016/s0020-7683(01)00035-x).
- 491 [13] Trojah, w., E. Streit, H.A. Chin, and D. Ehlert. n.d. Review of Progress in Bearing  
492 Performance of Advanced Nitrogen Alloyed Stainless Steel, Cronidur 30. Edited by  
493 FAG, OEM and Handel GmbH, Schweinfurt, Germany, FAG Aircraft and Super Precision  
494 Bearings GmbH, Schweinfurt, Germany, and Pratt and Whitney, Government Engine

495        & Space Propulsion Division, West Palm Beach, Florida. *Werkstofftech* 30: 605–11.  
496        Accessed October 30, 1999.

497 [14]    Hsieh, Chen, and Y.-C. Pan. 2000. “Dynamic Behavior and Modelling of the Pre-  
498        Sliding Static Friction.” *Wear* 242 (1-2): 1–17. <https://doi.org/10.1016/s0043->  
499        1648(00)00399-9.

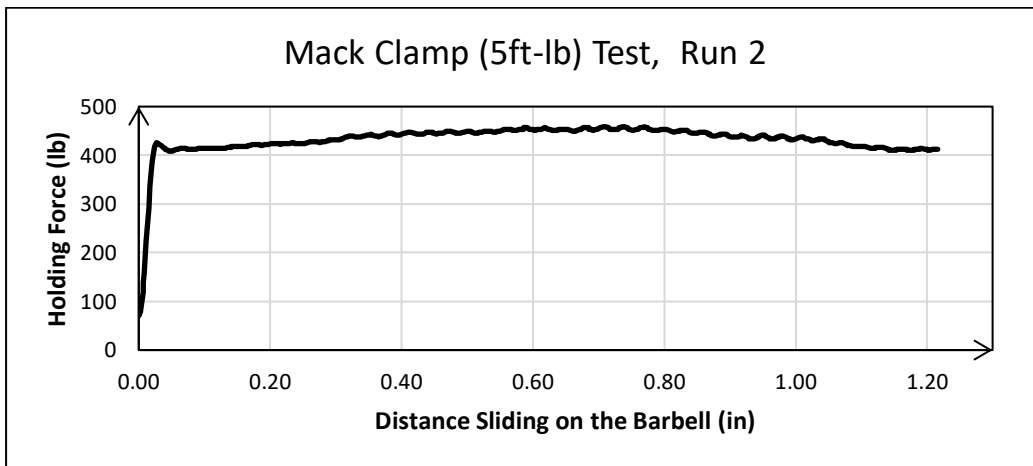
500

**Appendix A: Testing Graphs and Drawings**



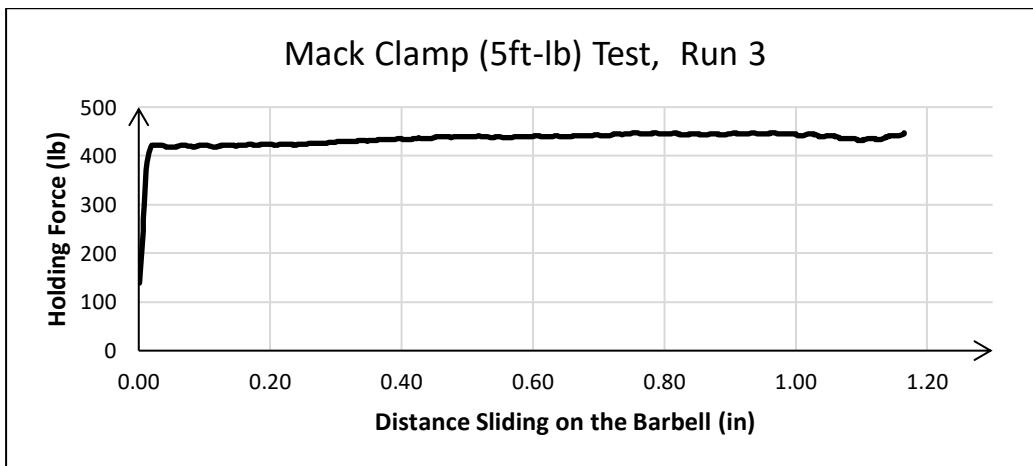
501  
502

Graph 3- Mack Clamp 5ft-lb, Run 1



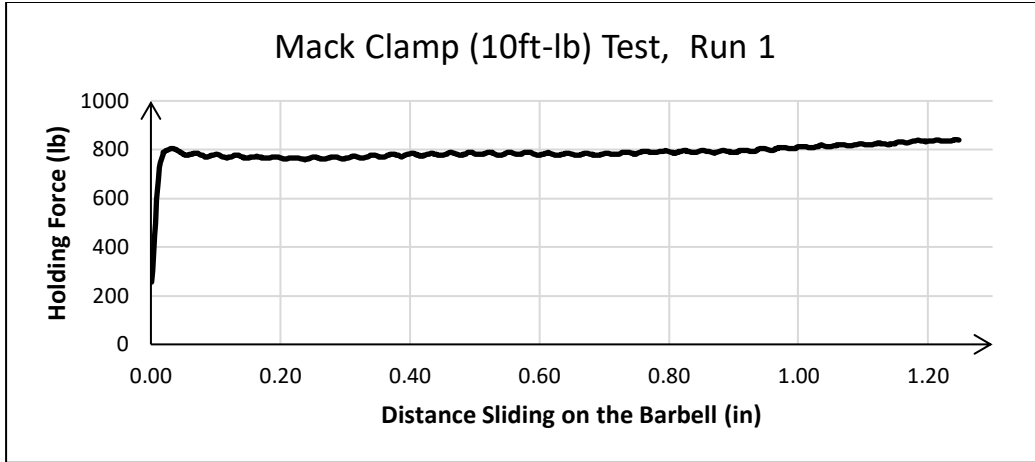
503  
504

Graph 4 – Mack Clamp 5ft-lb, Run 2



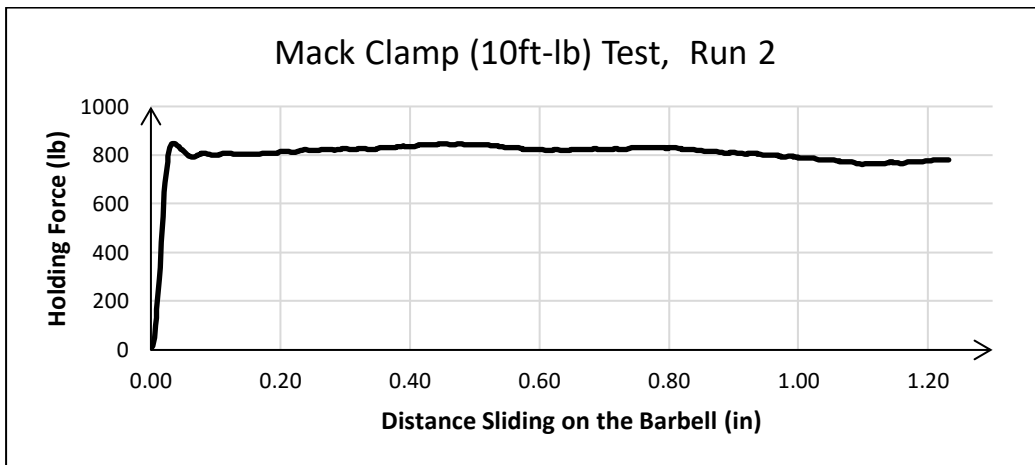
505  
506

Graph 5 – Mack Clamp 5ft-lb, Run 3



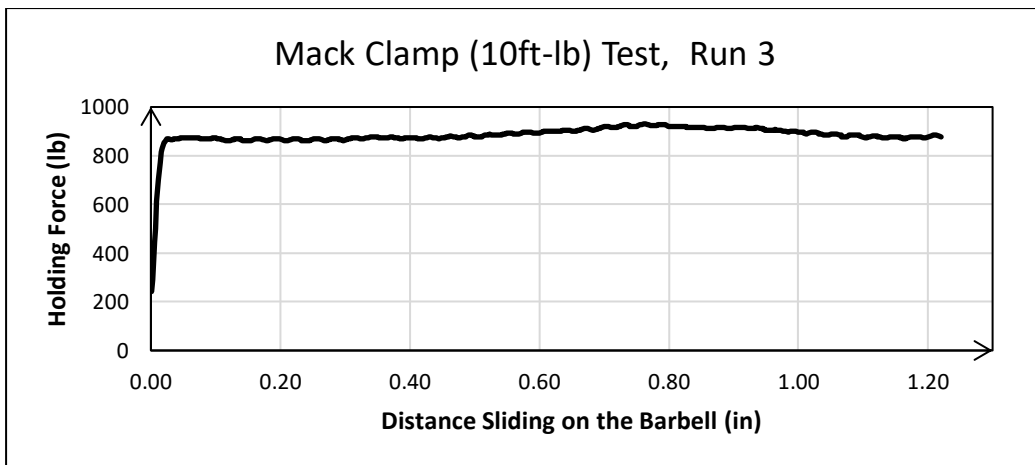
507  
508

Graph 6 – Mack Clamp 10ft-lb, Run 1



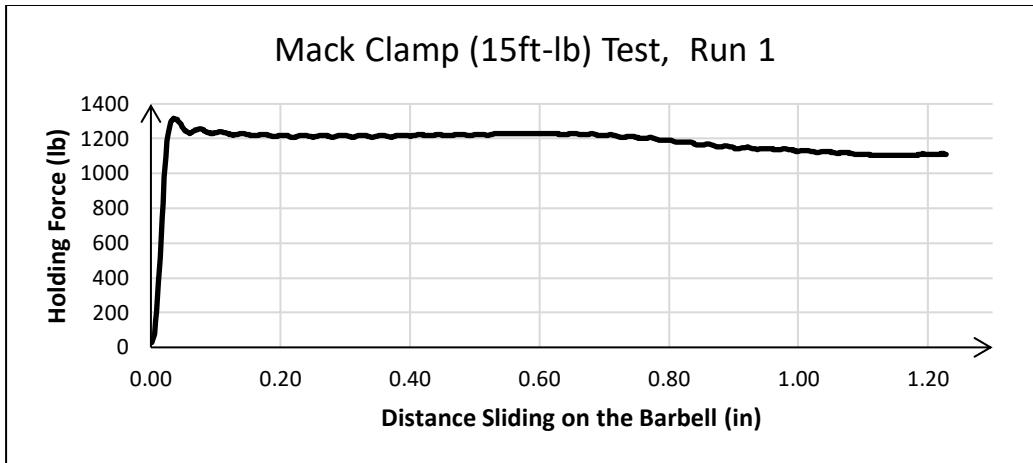
509  
510

Graph 7 – Mack Clamp 10ft-lb, Run 2



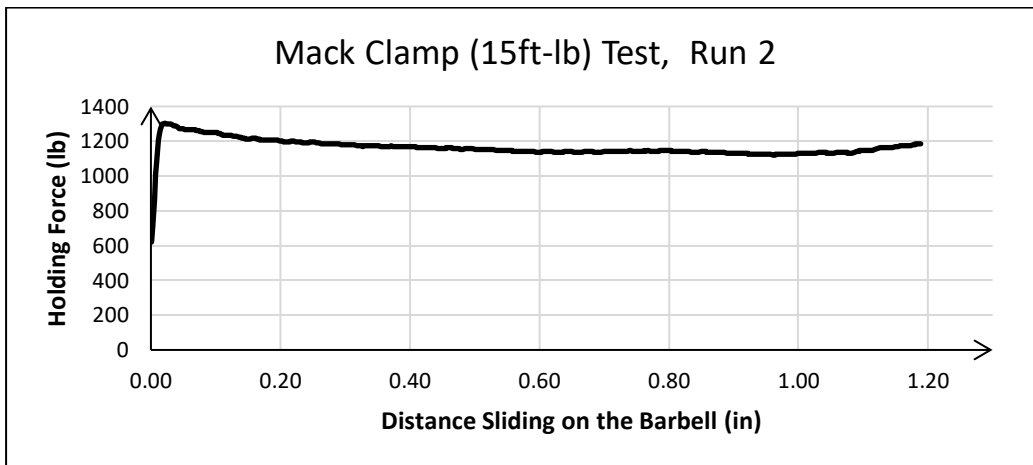
511  
512

Graph 8 – Mack Clamp 10ft-lb, Run 3



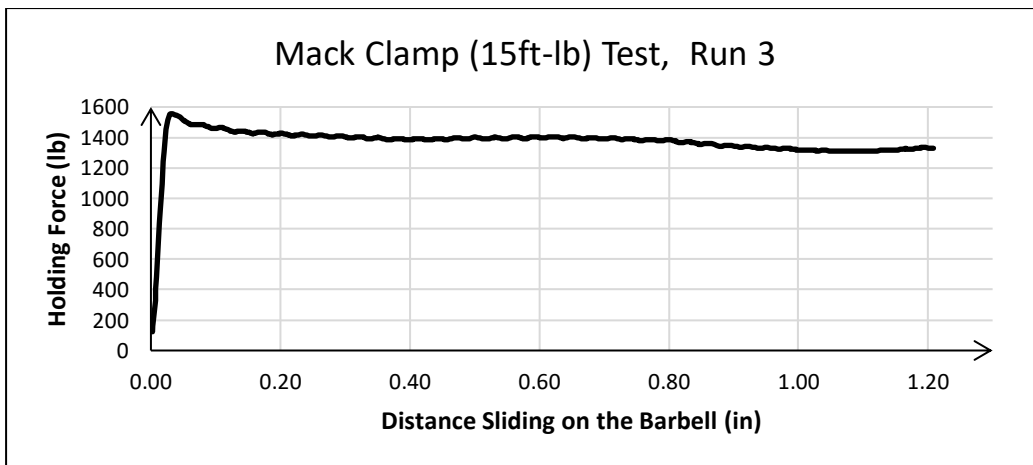
513  
514

Graph 9– Mack Clamp 15ft-lb, Run 1



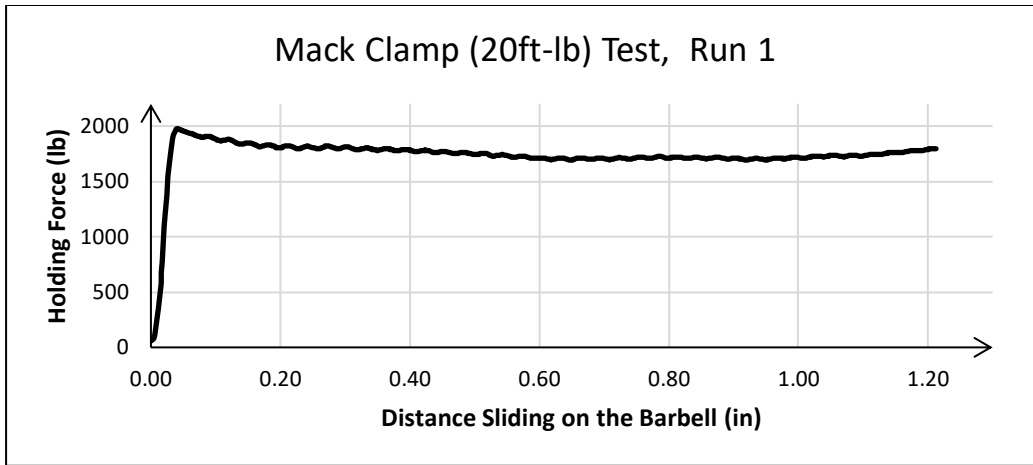
515  
516

Graph 10– Mack Clamp 15ft-lb, Run 2



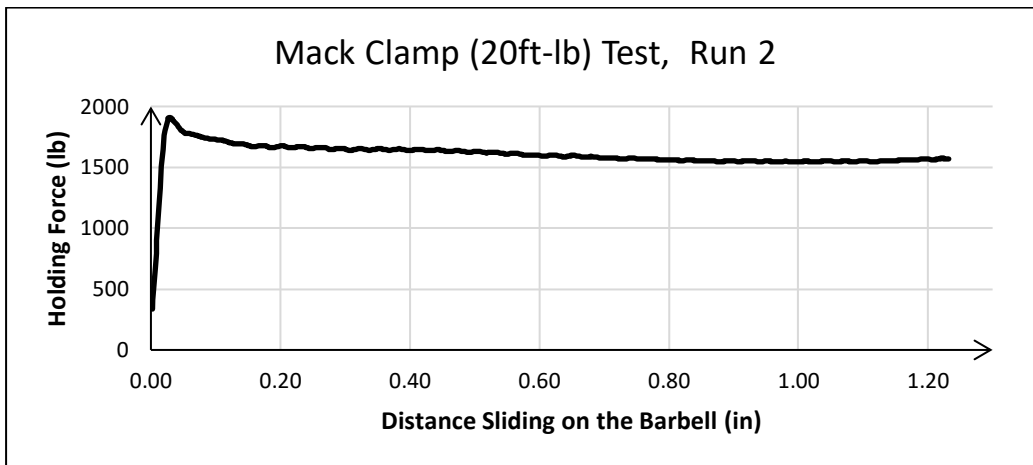
517  
518

Graph 11– Mack Clamp 15ft-lb, Run 3



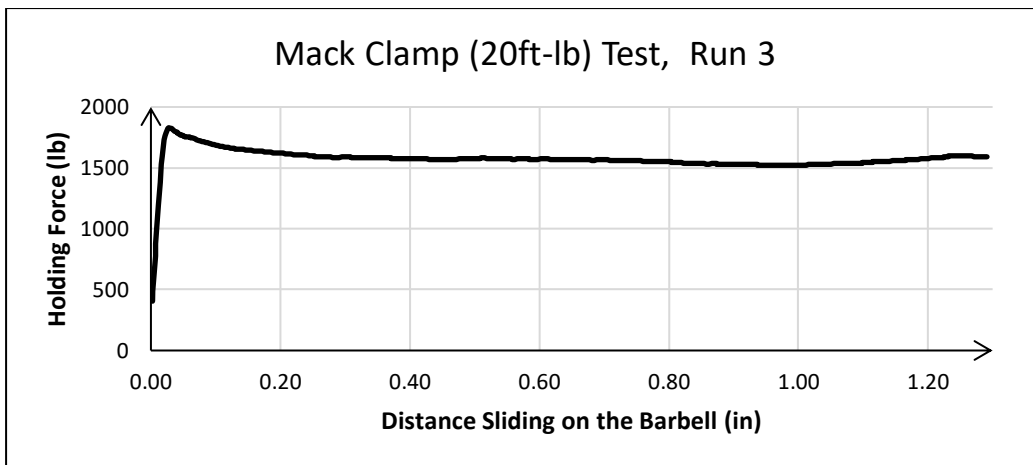
519  
520

Graph 12– Mack Clamp 20ft-lb, Run 1



521  
522

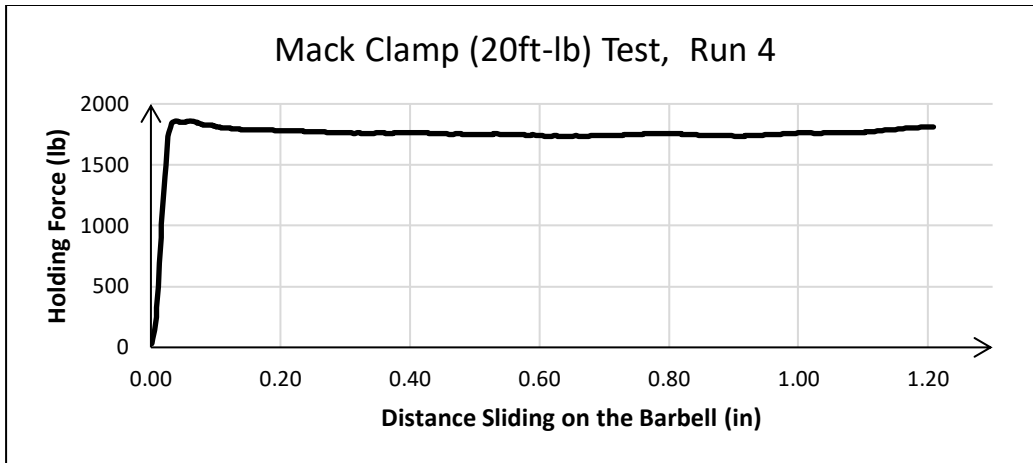
Graph 13– Mack Clamp 20ft-lb, Run 2



523  
524

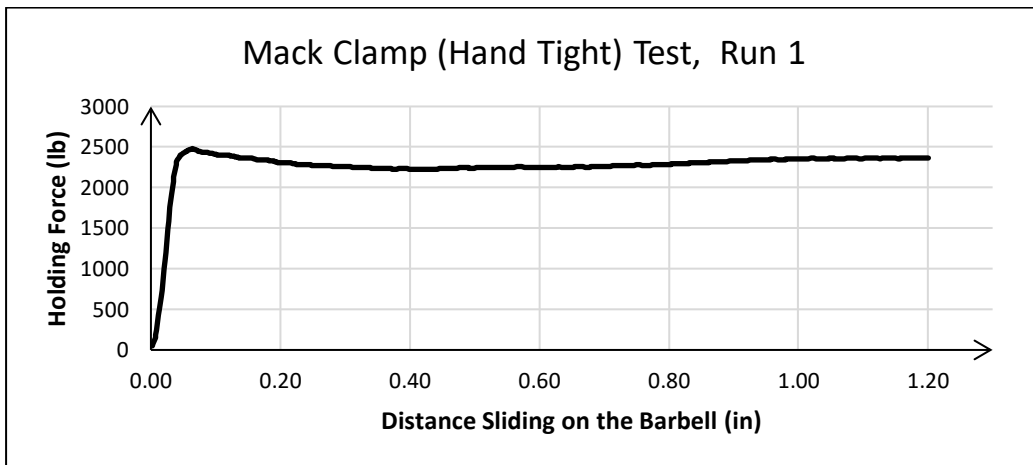
Graph 14– Mack Clamp 20ft-lb, Run 3





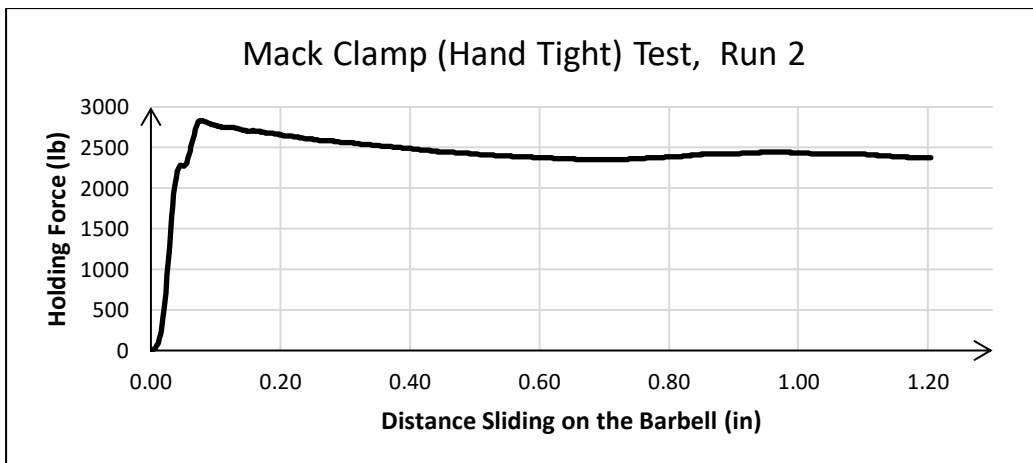
525  
526

Graph 15– Mack Clamp 20ft-lb, Run 4



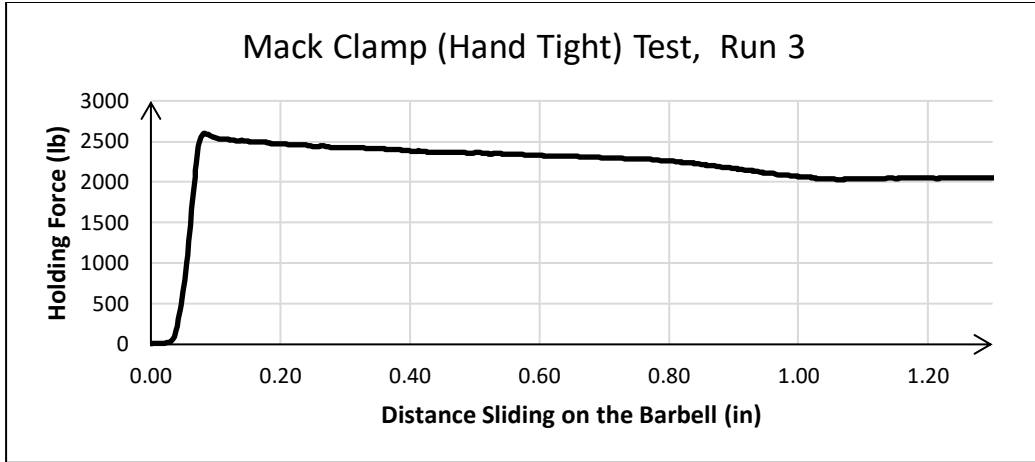
527  
528

Graph 16– Mack Clamp (Hand Tight), Run 1



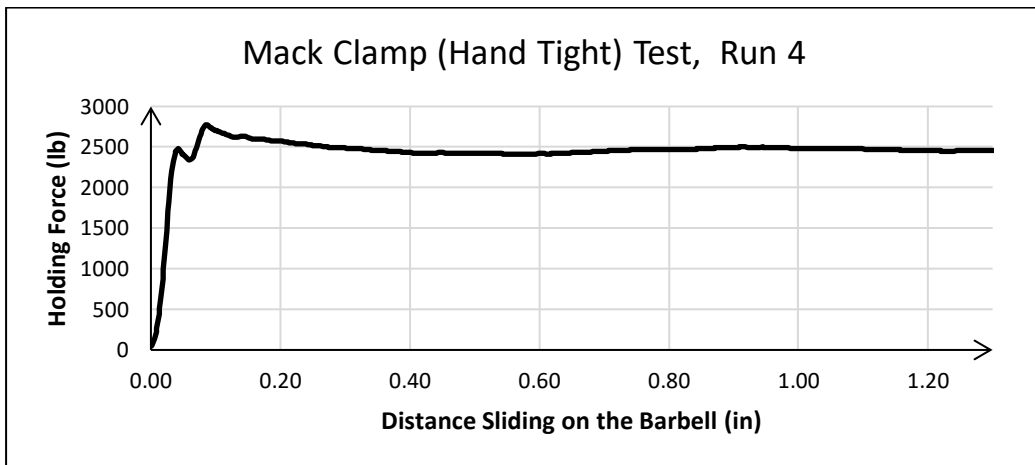
529  
530

Graph 17– Mack Clamp (Hand Tight), Run 2



531  
532

Graph 18– Mack Clamp (Hand Tight), Run 3



533  
534

Graph 19– Mack Clamp (Hand Tight), Run 4

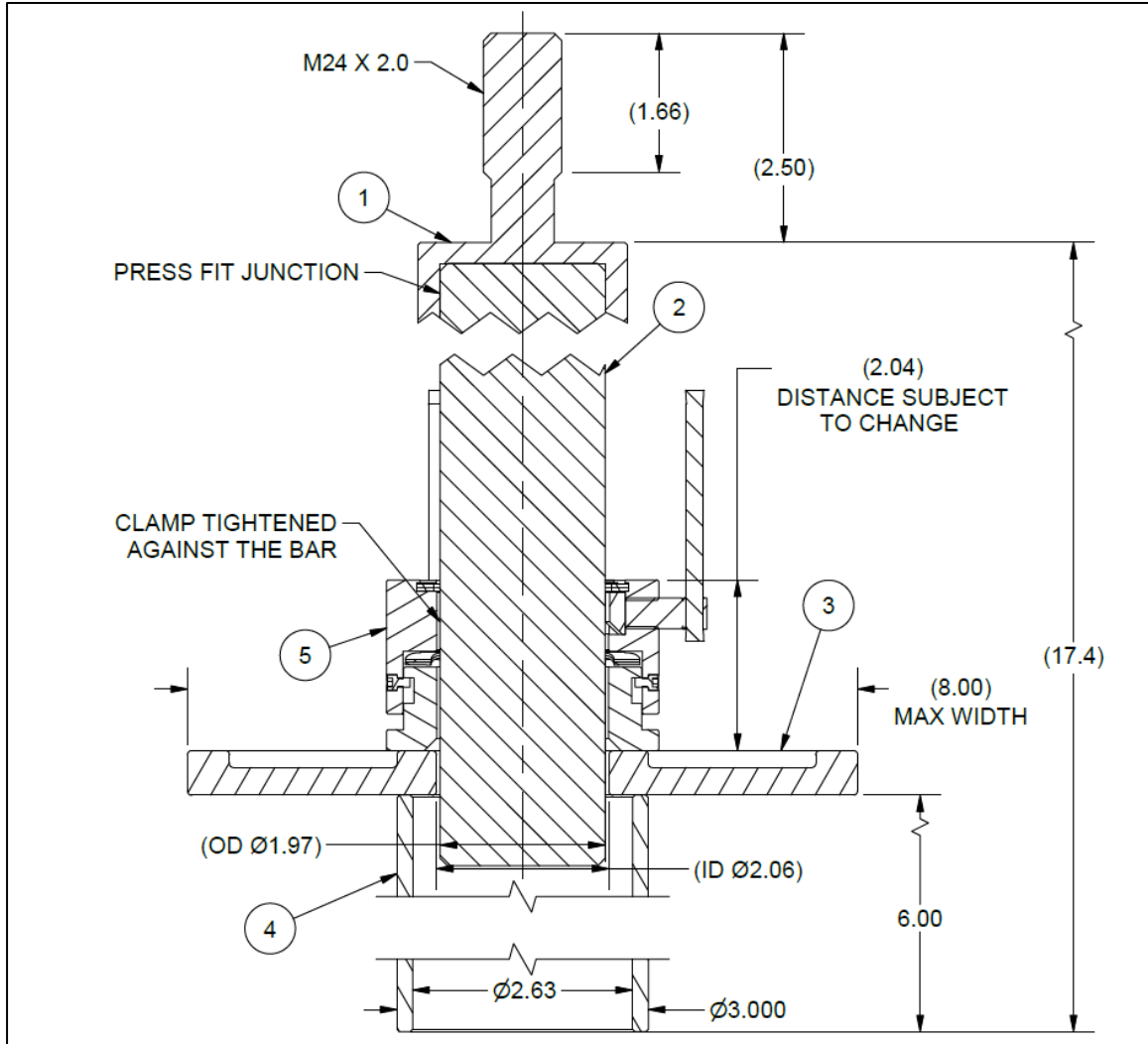


Figure 20. Weight Plate Retention Collar Testing Setup

535  
536

537

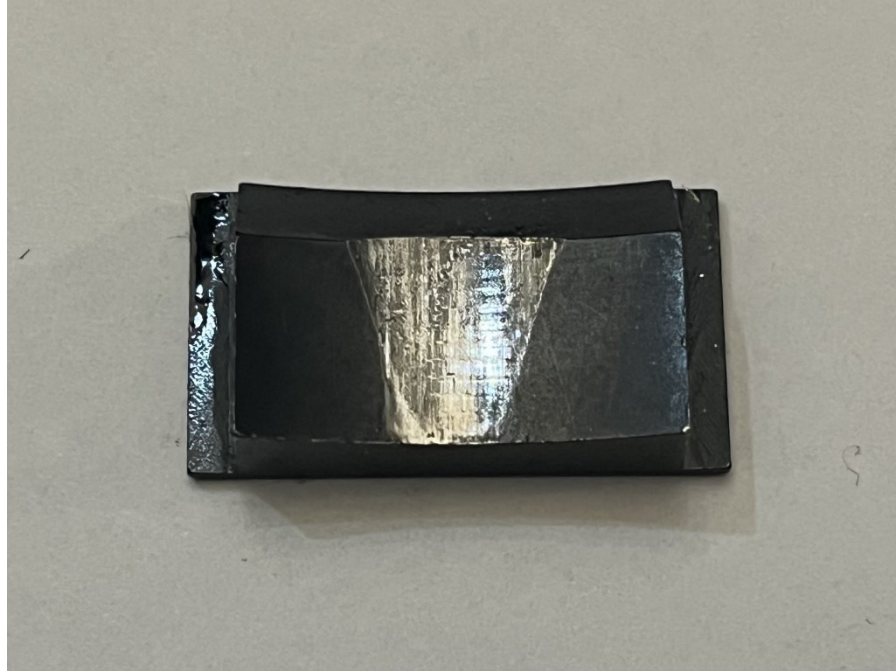


Figure 21. Contact Patch Closeup Post Testing

538  
539

540

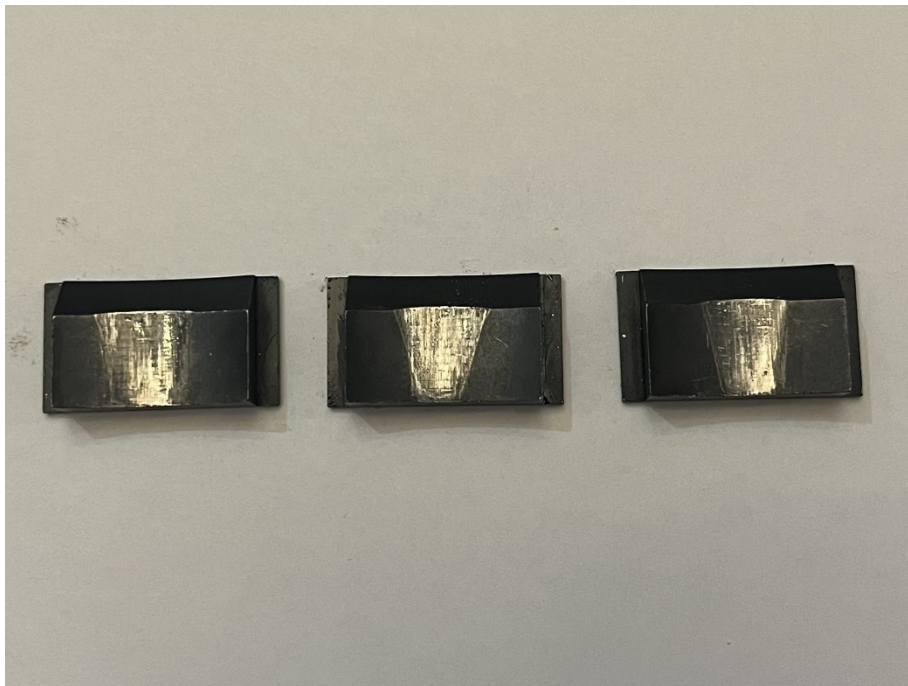
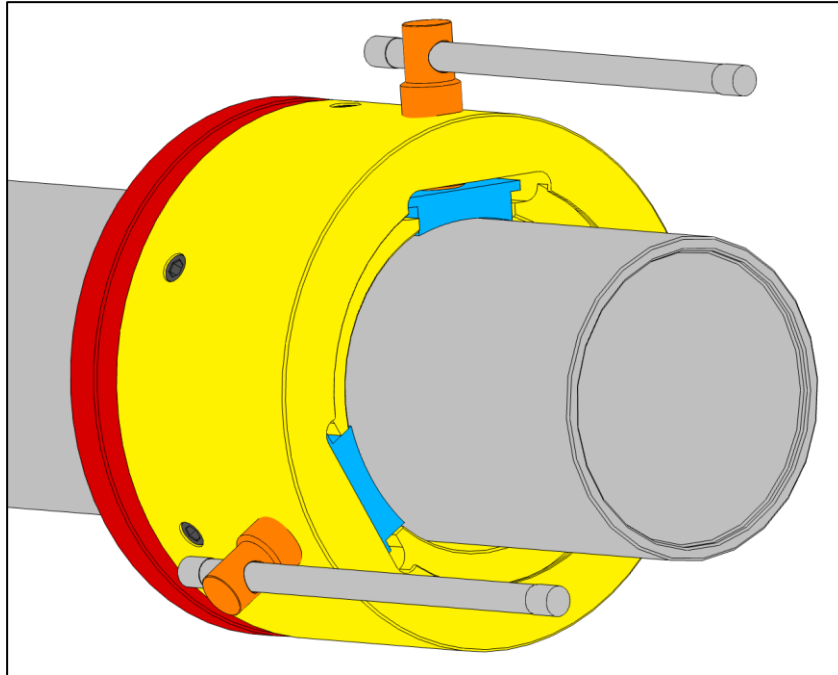


Figure 22. All three Contact Patches post testing

541  
542

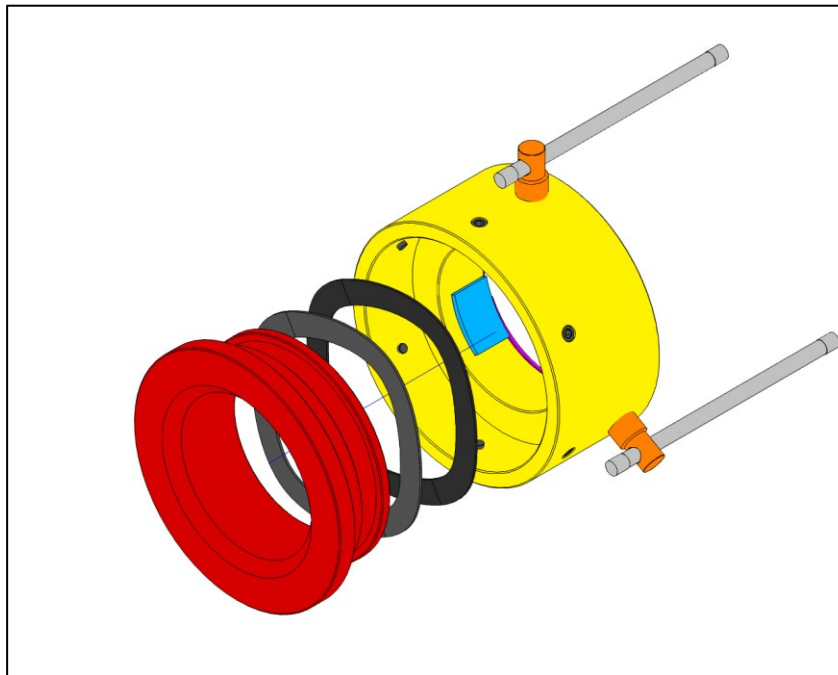
543

**Appendix B: Mack Clamp Illustrations**



544  
545

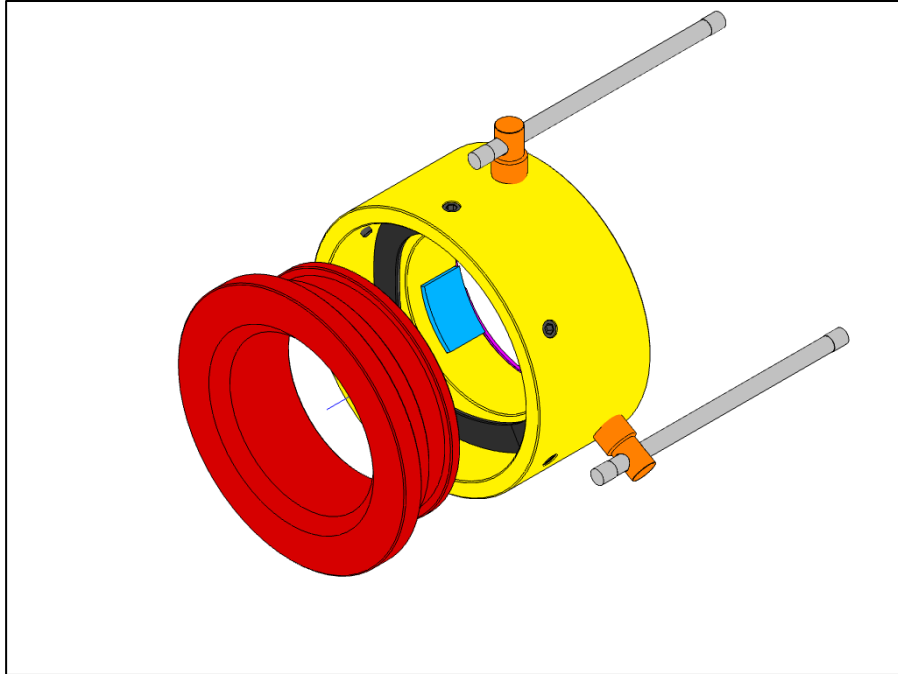
Figure 23. Mack Clamp Tightened onto a barbell sleeve



546  
547

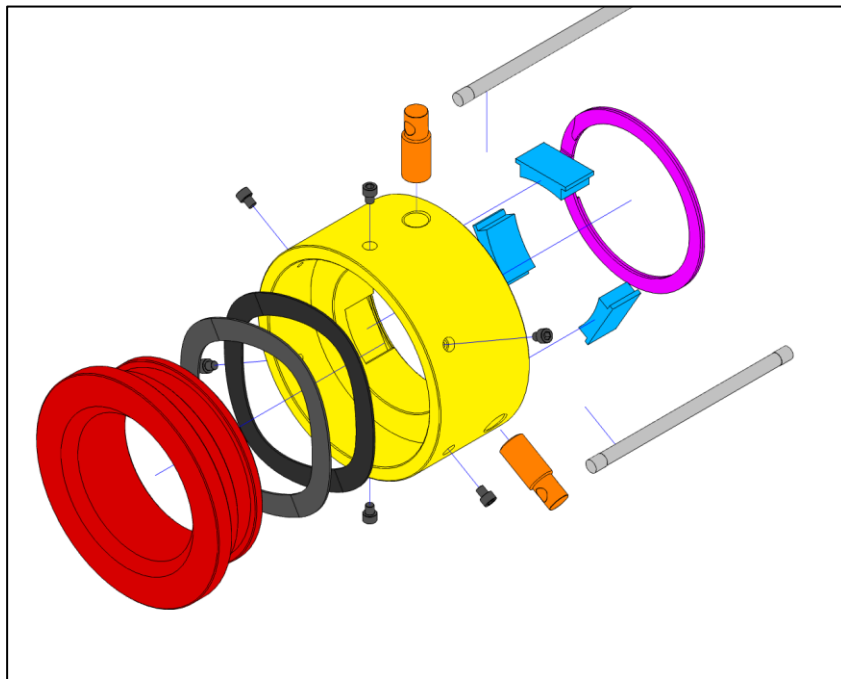
Figure 24. Mack Clamp Dynamic Shock Absorption system

548



549  
550

Figure 25. Mack Clamp Rotational Degree of Freedom



551  
552

Figure 26. Mack Clamp Explode View